Variable-Temperature and -Pressure Multinuclear Magnetic Resonance Studies on Solvent Exchange of Cobalt(II), Iron(II), and Manganese(II) Ions in Ethylenediamine. Kinetic Chelate Effect and Chelate Strain Effect

Sen-ichi Aizawa, Kayoko Matsuda, Tomomi Tajima, Machiyo Maeda, Takashi Sugata, and Shigenobu Funahashi*

Laboratory of Analytical Chemistry, Faculty of Science, Nagoya University, Chikusa, Nagoya 464-01, Japan

Received November 1, 1994[⊗]

Variable-temperature and -pressure NMR measurements of ethylenediamine exchange on Co^{2+}, Fe^{2+}, and Mn^{2+} in neat ethylenediamine (en) as a bidentate solvent have been performed by the ^{14}N, ^{13}C, and ^{1}H NMR line-broadening technique. The solvent exchange rate constant at 298 K (k_{ex}^{298}/s^{-1}), activation enthalpy ($\Delta H^{\ddagger}$/kJ mol^{-1}), activation entropy ($\Delta S^{\ddagger}$/J mol^{-1} K^{-1}), and activation volume ($\Delta V^{\ddagger}$/cm^3 mol^{-1}) for the ethylenediamine exchange reaction on each metal ion are respectively as follows: 5.4×10^3, 56.5 ± 3.3, 16 ± 10, and 0.9 ± 0.9 for Co^{2+}; 4.3×10^4, 46.3 ± 1.4, -1 ± 4, and -1.2 ± 0.8 for Fe^{2+}; 1.7×10^6, 24.7 ± 1.6, -43 ± 5, and -0.6 ± 0.5 for Mn^{2+}. The exchange rate constants are smaller than available rate constants in monodentate solvents for the corresponding metal(II) ions. The variation in values of k_{ex}^{298} and $\Delta H^{\ddagger}$ for the en exchange along the series from Ni^{2+} to Mn^{2+} is more drastic than that for monodentate solvent exchange. The values of $\Delta V^{\ddagger}$ in en indicate no changeover of the mechanism from a dissociative interchange (I_d) for Ni^{2+} to an associative interchange (I_a) for Mn^{2+} as observed for monodentate solvent exchange. Such characteristic features for en exchange have been explained in terms of the chelate effect and chelate strain effect of the bidentate en molecule.

Introduction

Solvent exchange reactions of the transition metal ions have been extensively studied as fundamental reactions to understand the kinetics of complex formation.[1−26] These studies have revealed that the reaction mechanism of solvent exchange mainly depends on the metal ions although the exchange rate is affected by the electronic and steric properties of solvents.[23] Merbach et al. have rationalized a gradual changeover of the mechanism along the first-row transition metal series by means of a change in the ionic radius and the t_{2g} orbital occupancy.[23] These results have been obtained from studies for monodentate solvents such as water, methanol, and acetonitrile. We have extended the solvent exchange study to solvent exchange reactions in ethylenediamine (en) which potentially possesses chelating ability.

The results previously obtained for en exchange on Ni^{2+} indicated a dissociative mechanism with a positive activation volume comparable to those for some monodentate solvents.[27] Therefore, it is desirable to confirm whether the mechanistic changeover is also observed for bidentate solvent exchange for the first-row transition metal(II) series. In addition, an extremely slow rate was previously observed for en exchange on Ni^{2+} probably due to a chelate effect.[27] However, so far there has not been a rational explanation for its origin. Because the chelate effect is expected to be sensitive to metal ion size relative to a chelate ring size, studies for a series of metal ions with different ion radii will provide insight into the chelate effect on solvent exchange. Furthermore, there are a great number of available structural data for en complexes ($[M(en)_3]^{n+}$) to permit a comparison of the structures of the ground state and the transition state for en exchange. Accordingly, we have extended the en exchange studies to the divalent first-row

[⊗] Abstract published in *Advance ACS Abstracts,* March 15, 1995.

(1) Burgess, J. *Metal Ions in Solution*; Ellis Horwood: New York, 1978.
(2) Swaddle, T. W.; Stranks, D. R. *J. Am. Chem. Soc.* **1972**, *94*, 8357.
(3) Tong, S. B.; Swaddle, T. W. *Inorg. Chem.* **1974**, *13*, 1538.
(4) Swaddle, T. W. *Coord. Chem. Rev.* **1974**, *14*, 217.
(5) Merbach, A. E.; Vanni, H. *Helv. Chim. Acta* **1977**, *60*, 1124.
(6) Earl, W. L.; Meyer, F. K.; Merbach, A. E. *Inorg. Chim. Acta* **1977**, *25*, L91.
(7) Funahashi, S.; Nishimoto, T.; Hioki, A.; Tanaka, M. *Inorg. Chem.* **1981**, *20*, 2648.
(8) Meyer, F. K.; Earl, W. L.; Merbach, A. E. *Inorg. Chem.* **1979**, *18*, 888.
(9) Meyer, F. K.; Newman, K. E.; Merbach, A. E. *Inorg. Chem.* **1979**, *18*, 2142.
(10) Vanni, H.; Merbach, A. E. *Inorg. Chem.* **1979**, *18*, 2758.
(11) Ducommun, Y.; Earl, W. L.; Merbach, A. E. *Inorg. Chem.* **1979**, *18*, 2754.
(12) Newman, K. E.; Meyer, F. K.; Merbach, A. E. *J. Am. Chem. Soc.* **1979**, *101*, 1470.
(13) Meyer, F. K.; Newman, K. E.; Merbach, A. E. *J. Am. Chem. Soc.* **1979**, *101*, 5588.
(14) Ducommun, Y.; Newman, K. E.; Merbach, A. E. *Inorg. Chem.* **1980**, *19*, 3696.
(15) Grant, M.; Jordan, R. B. *Inorg. Chem.* **1981**, *20*, 55.
(16) Swaddle, T. W.; Merbach, A. E. *Inorg. Chem.* **1981**, *20*, 4212.
(17) Ducommun, Y.; Zbinden, D.; Merbach, A. E. *Helv. Chim. Acta* **1982**, *65*, 1385.
(18) Xu, F.-C.; Krouse, H. R.; Swaddle, T. W. *Inorg. Chem.* **1985**, *24*, 267.
(19) Helm, L.; Elding, L. I.; Merbach, A. E. *Inorg. Chem.* **1985**, *24*, 1719.
(20) Hugi, A. D.; Helm, L.; Merbach, A. E. *Helv. Chim. Acta* **1985**, *68*, 508.
(21) Hugi, A. D.; Helm, L.; Merbach, A. E. *Inorg. Chem.* **1987**, *26*, 1763.
(22) Li, C.; Jordan, R. B. *Inorg. Chem.* **1987**, *26*, 3855.
(23) Merbach, A. E. In *High Pressure Chemistry and Biochemistry*; van Eldik, R., Jonas, J., Eds.; D. Reidel Publishing: Dordrecht, The Netherlands, 1987; pp 311−331.
(24) Rapaport, I.; Helm, L.; Merbach, A. E.; Bernhard, P.; Ludi, A. *Inorg. Chem.* **1988**, *27*, 873.
(25) (a) Ishii, M.; Funahashi, S.; Tanaka, M. *Inorg. Chem.* **1988**, *27*, 3192. (b) Hioki, A.; Funahashi, S.; Ishii, M.; Tanaka, M. *Inorg. Chem.* **1986**, *25*, 1360. (c) Hioki, A.; Funahashi, S.; Tanaka, M. *Inorg. Chem.* **1986**, *25*, 2904.
(26) Ishii, M.; Funahashi, S.; Ishihara, K.; Tanaka, M. *Bull. Chem. Soc. Jpn.* **1989**, *62*, 1852.
(27) Soyama, S.; Ishii, M.; Funahashi, S.; Tanaka, M. *Inorg. Chem.* **1992**, *31*, 536.

0020-1669/95/1334-2042$09.00/0

transition metal ions, Co^{2+}, Fe^{2+}, and Mn^{2+}, and report here the kinetic results with reference to stereochemical aspects.

Experimental Section

Solvents. Ethylenediamine (en) was purified by the same procedure as previously described.[27] Reagent grade *N,N*-dimethylformamide (DMF) was dried over activated 4A molecular sieves and distilled twice under reduced pressure.

$[Co(H_2O)_6](CF_3SO_3)_2$. $CoCl_2 \cdot 6H_2O$ (Wako, Special Grade) was dissolved in an aqueous solution of trifluoromethanesulfonic acid (triflic acid, Wako, 98%). The solution was concentrated under an infrared lamp. The dissolution–concentration procedure was repeated to completely remove HCl. Finally, reddish crystals were obtained by filtration.

$[Fe(H_2O)_6](CF_3SO_3)_2$ and $Mn(CF_3SO_3)_2$. Iron Sponge (Wako, 99.99%) and $MnCO_3$ (Wako) were respectively added to an aqueous solution of triflic acid. Each mixture was heated to complete the reaction, and the residue was filtered off. The filtrate was cooled to obtain the crystals. All the procedures were carried out under argon. The hydrated manganese(II) triflate was dried at 280 °C for 2 h to obtain the anhydrous salt.

$[M(en)_3](CF_3SO_3)_2$ (M = Co(II), Fe(II), Mn(II). The purified en was transferred over $[M(H_2O)_6](CF_3SO_3)_2$ by distillation in a vacuum line, and then the en solution of the metal(II) ion was concentrated under reduced pressure to remove the water. The distillation–concentration procedure was repeated twice. Crystals for the Co(II) and Fe(II) complexes were collected by filtration under an argon atmosphere. The Mn(II) complex was obtained by concentration to dryness. Anal. Calcd for $[Co(en)_3](CF_3SO_3)_2$: C, 17.88; H, 4.47; N, 15.64. Found: C, 18.01; H, 4.48; N, 15.63. UV/vis (in en), λ_{max}/nm (ϵ/kg mol^{-1} cm^{-1}): 485 (10.8), 1003 (3.8) for Co(II); 861 (1.9), 1000 sh (1.8) for Fe(II); 356 (0.63), 376 (0.57), 422 (0.53), 502 (0.39), 636 (0.28) for Mn(II).

Sample Preparation. Sample preparations for NMR measurements were carried out in a glovebox by using freshly distilled en. Sample solutions of the Co(II) ion were prepared by dissolving weighed quantities of $[Co(en)_3](CF_3SO_3)_2$ in a suitable amount of en. The stock solutions for Fe^{2+} and Mn^{2+} were prepared by dissolving $[Fe(en)_3](CF_3SO_3)_2$ and $Mn(CF_3SO_3)_2$ or $[Mn(en)_3](CF_3SO_3)_2$ in en, respectively. The concentrations of Fe^{2+} and Mn^{2+} in the stock solutions were determined by colorimetry with phenanthroline[28] and by EDTA titration with BT (1-(1-hydroxy-2-naphthylazo)-6-nitro-2-naphthol-4-sulfonic acid, sodium salt) as an indicator,[29] respectively. The compositions of sample solutions are given in Table S1 (supplementary material). Sample solutions for variable-temperature NMR measurements were introduced into 5 mm o.d. NMR glass tubes that were then flame-sealed after degassing in a vacuum line. The variable-pressure NMR sample solutions were transferred into 7 mm o.d. NMR tubes, each capped with a flexible Teflon tube, as previously described.[25,26]

NMR Measurements. The ^{14}N, ^{13}C, and ^{1}H NMR measurements at various temperatures were performed on a JEOL JNM-GX 270 FT-NMR spectrometer operating at 19.52, 67.89, and 270.05 MHz, respectively. A JEOL JMN-FX 100 FT-NMR spectrometer was also used to observe the frequency dependence of the relaxation rate. A 5 mm o.d. NMR sample tube for ^{13}C and ^{14}N NMR measurements was inserted into a 10 mm o.d. NMR tube containing a lock solvent (D_2O and/or deuterated ethylene glycol). The temperature was measured by a substitution technique using a thermistor (D641, Takara Thermistor Co.). About 15–30 min was required for the temperature equilibration of the sample solution, and the temperature stability was ±0.1 K.

The NMR measurements at various pressures were carried out by using a high-pressure NMR probe constructed for the wide-bore superconducting magnet (6.34 T) of a JEOL JNM-GX270 FT-NMR spectrometer.[26] The pressure generated by a pressure-generating pump (KBP56, Hikarikouatsu Co., Hiroshima) was measured with a Heise Bourdon gauge. Daifloil No. 1 (poly(chlorotrifluoroethylene), Daikin-kogyo Co.) was used as a pressure-transmitting liquid. The temperature of the sample solution was measured by a substitution technique with a thermistor before the high-pressure measurements and monitored with a thermocouple introduced into the pressure vessel during the high-pressure experiments. About 5–8 h was required for the complete temperature equilibration, and the temperature stability was ±0.2 K. The electronic absorption spectra of en solutions of Co(II), Fe(II), and Mn(II) ions were recorded on a Shimadzu UV-265 FW spectrophotometer.

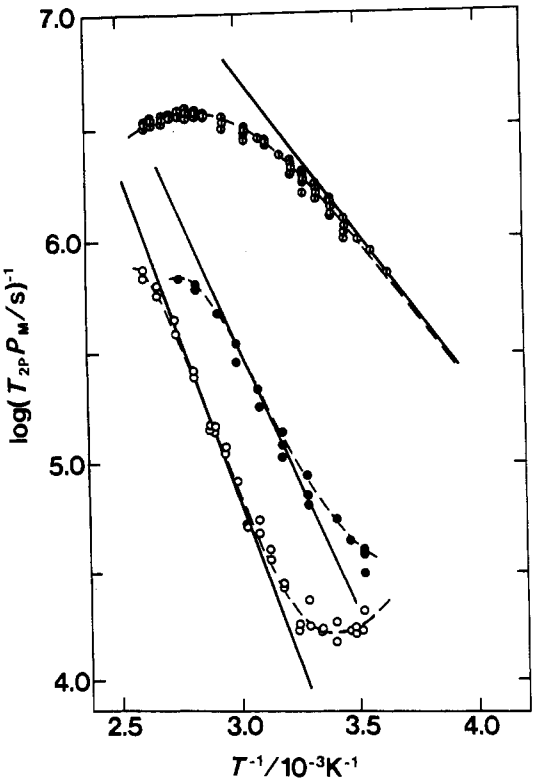

Figure 1. Temperature dependence of $\log(T_{2P}P_M)^{-1}$ for 19.52-MHz ^{14}N NMR. Co^{2+} (○): $P_M = 5.28 \times 10^{-3}$, 9.17×10^{-3}, 1.68×10^{-2}, 3.46×10^{-2}. Fe^{2+} (●): $P_M = 4.03 \times 10^{-3}$, 7.01×10^{-3}, 1.15×10^{-2}. Mn^{2+} (Φ): 7.29×10^{-4}, 8.03×10^{-4}, 1.28×10^{-3}, 5.55×10^{-3}, 6.75×10^{-3}, 5.07×10^{-4} (70% en). The solid line indicates the contribution of τ_M^{-1}.

Results

Variable-Temperature NMR Study. The visible absorption spectra for neat en solutions of Co^{2+} and Mn^{2+} are in good agreement with those for the solid states of $[Co(en)_3](NO_3)_2$[30] and $[Mn(en)_3](NO_3)_2$,[31] respectively. The en solution of Fe^{2+} exhibits a splitting absorption band around 1.16×10^4 and 1.00×10^4 cm^{-1} due to the d–d transition from the $^5T_{2g}$ to the ^5E_g state, which is characteristic of octahedral high-spin iron(II) complexes.[32] These findings confirm that each metal(II) (M(II)) ion forms the paramagnetic tris(ethylenediamine) complex ($[M(en)_3]^{2+}$) in an en solution.

The NMR line broadening, $(T_{2P}P_M)^{-1}$, of solvent molecules in the bulk due to the paramagnetic ion is expressed as $(T_{2P}P_M)^{-1} = \pi(\Delta\nu_{obsd} - \Delta\nu_{solv})P_M^{-1}$, where $\Delta\nu_{obsd}$ and $\Delta\nu_{solv}$ are the half-height widths of the NMR spectra of the solvent molecules in the bulk in the presence and absence, respectively, of the paramagnetic ion. T_{2P} is the transverse relaxation time, and P_M is the mole fraction of bound solvent molecules. Figure 1 shows the temperature dependences of $(T_{2P}P_M)^{-1}$ for ^{14}N of ethylenediamine in the bulk for three metal ions, Co^{2+}, Fe^{2+}, and Mn^{2+}. The temperature dependences of $(T_{2P}P_M)^{-1}$ for three different nuclei (^{14}N, ^{13}C, and ^{1}H) of en at various frequencies

(28) Day, R. A.; Underwood, A. L. *Quantitative Analysis*; Prentice-Hall: Englewood Cliffs, NJ, 1967.
(29) Flaschka, H.; Amin, A. M. *Mikrochim. Acta* **1953**, 330.
(30) Yang, M. C.-L.; Palmer, R. A. *J. Am. Chem. Soc.* **1975**, *97*, 5390.
(31) Palmer, R. A.; Yang, M. C.-L.; Hempel, J. C. *Inorg. Chem.* **1978**, *17*, 1200.
(32) Lever, A. B. P. *Inorganic Electronic Spectroscopy*; Elsevier: Amsterdam, 1984; pp 458–462.

are given in Figures S1–S3 (supplementary material), and all the line broadening data are deposited in Tables S2–S4. In each case, the observed transverse relaxation rate, T_{2P}^{-1}, has been confirmed to be proportional to the P_M value. Thus, the T_{2P}^{-1} value can be normalized by dividing by P_M. These NMR line broadening data were analyzed by means of the modified Swift–Connick equation:[33,34]

$$\frac{1}{T_{2P}P_M} = \frac{1}{\tau_M}\frac{T_{2M}^{-2} + (\tau_M T_{2M})^{-1} + (\Delta\omega_M)^2}{(\tau_M^{-1} + T_{2M}^{-1})^2 + (\Delta\omega_M)^2} + \frac{1}{T_{2o}} \quad (1)$$

in which the symbols have their usual meanings.[35] The solvent exchange rate constant k_{ex} is equal to $\tau_M^{-1} = (k_B T/h)\exp(-\Delta H^{\ddagger}/RT + \Delta S^{\ddagger}/R)$. The temperature dependence of $\Delta\omega_M$ is given by $\Delta\omega_M = -C_\omega/T$. $T_{2M}^{-1} = (C_M/T)\exp(E_M/RT)$ and T_{2o} is also expressed as $T_{2o}^{-1} = (C_o/T)\exp(E_o/RT)$.[34] When T_{2M}^{-1} is small enough compared with the other relaxation term, eq 1 is reduced to

$$(T_{2P}P_M)^{-1} = 1/(\tau_M^{-1}(\Delta\omega_M)^{-2} + \tau_M) + T_{2o}^{-1} \quad (2)$$

When T_{2o}^{-1} is negligible, eq 2 becomes

$$(T_{2P}P_M)^{-1} = 1/(\tau_M^{-1}(\Delta\omega_M)^{-2} + \tau_M) \quad (3)$$

For $T_{2M}^{-2} \gg (\Delta\omega_M)^2$, T_{2o}^{-1}, eq 1 is reduced to

$$(T_{2P}P_M)^{-1} = 1/(T_{2M} + \tau_M) \quad (4)$$

For the line-broadening data for Co^{2+} and Fe^{2+}, the frequency dependence region with the $\tau_M(\Delta\omega_M)^2$ term and the chemical exchange region with the τ_M^{-1} term were observed. Among these line-broadening data, nonlinear least-squares analyses according to eq 2 were applied to the data of 19.52-MHz ^{14}N NMR and 270.05-MHz ^1H NMR for Co^{2+}, because the temperature region in which the T_{2o}^{-1} term predominates was observed. The other data for Co^{2+} and Fe^{2+} were analyzed by means of eq 3. The line-broadening data of 19.52- and 7.15-MHz ^{14}N NMR for Mn^{2+} were analyzed by means of eq 4, because both the region in which the T_{2M}^{-1} term predominates without frequency dependence and the chemical exchange region were observed. The ^1H and ^{13}C NMR data for Mn^{2+}, which did not sufficiently contain chemical exchange contributions, were analyzed with fixed $\Delta H^{\ddagger}$ and $\Delta S^{\ddagger}$ values obtained from the ^{14}N NMR data for Mn^{2+}. Nearly the same values of the activation parameters for the en exchange were obtained from the NMR data of the different nuclei and observed frequencies for each metal ion. The activation parameters and rate constants were determined to be $\Delta H^{\ddagger} = 56.5 \pm 3.3$, 46.3 ± 1.4, and 24.7 ± 1.6 kJ mol^{-1}, $\Delta S^{\ddagger} = 16 \pm 10$, -1 ± 4, and -43 ± 5 J mol^{-1} K^{-1}, and $k_{ex}(25\ °C) = 5.4 \times 10^3$, 4.3×10^4, and 1.7×10^6 s^{-1}, for Co^{2+}, Fe^{2+}, and Mn^{2+}, respectively, from the 19.52-MHz ^{14}N NMR data. All the parameters obtained by least-squares fitting are summarized in Table S5.

In order to carry out the variable-pressure experiments for Mn^{2+} at lower temperatures where the chemical exchange predominates (vide infra), we have confirmed that the en exchange rate is independent of the concentration of en (100 and 70%) in DMF. Furthermore, no line broadening of ^{14}N NMR spectra of DMF, even in the presence of Mn^{2+}, has been observed (Table S4). The same findings were also obtained in the case of the en exchange for Ni^{2+} and Cu^{2+} as described previously.[27,36] Therefore, in the mixture of en and DMF, DMF molecules do not bind to the paramagnetic manganese(II) ion.

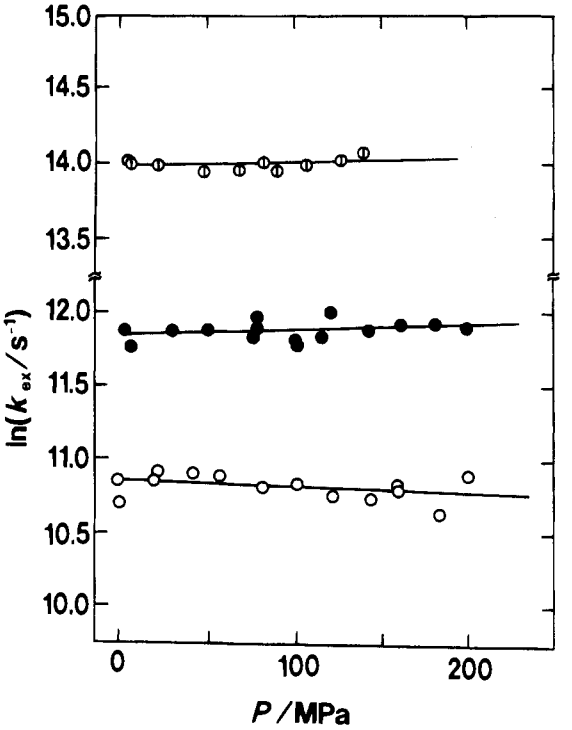

Figure 2. Pressure dependence of ln k_{ex} for en exchange on Co^{2+} at 332.4 K (○), Fe^{2+} at 324.5 K (●), and Mn^{2+} at 278.4 K (Φ).

Variable-Pressure NMR Study. The solid lines in Figure 1 represent the contribution of τ_M^{-1} for each metal ion. In the temperature range in which each curve overlaps with the solid line, $(T_{2P}P_M)^{-1}$ is equal to τ_M^{-1}, i.e., k_{ex}. Therefore, the variable-pressure ^{14}N NMR experiments have been performed at 332.4 and 324.5 K for Co^{2+} and Fe^{2+}, respectively. In the case of ^{14}N NMR for Mn^{2+}, the predominant chemical exchange region was not observed down to the freezing point of en, and the neat en solution was frozen at 298 K under 160 MPa. Therefore, the variable-pressure experiments were carried out in a 70% en solution diluted with DMF at 278.4 K where $(T_{2P}P_M)^{-1}$ corresponds to k_{ex} (vide supra). The pressure dependences of k_{ex} for three metal ions are shown in Figure 2, and the values of k_{ex} at various pressures are listed in Table S6. From the transition-state theory, the activation volume, $\Delta V^{\ddagger}$, is given by the relation, $(\partial \ln k_p/\partial P)_T = -\Delta V^{\ddagger}/RT$. Since plots of ln k_{ex} vs P are linear within experimental errors, the $\Delta V^{\ddagger}$ values were determined from the slopes to be 0.9 ± 0.9, -1.2 ± 0.8, and -0.6 ± 0.5 cm^3 mol^{-1} for Co^{2+}, Fe^{2+}, and Mn^{2+}, respectively.

Discussion

There have been numerous studies on solvent exchange in monodentate solvents such as water, methanol, acetonitrile, DMF, and acetic acid.[1–26] The rate constant, k_{ex}, and the activation parameters, $\Delta H^{\ddagger}$, $\Delta S^{\ddagger}$, and $\Delta V^{\ddagger}$, for water exchange on the divalent first-row transition metal ions are listed in Table 1 together with the results for the en exchange. The kinetic data for water exchange have some general trends along the transition-metal series as observed in the case of representative monodentate solvents, methanol, acetonitrile, and DMF.[37] First, k_{ex} increases in the following order: $Ni^{2+} < Co^{2+} < Fe^{2+} < Mn^{2+}$, with a decrease in the value of $\Delta H^{\ddagger}$. The trend of the

(33) Swift, T. J.; Connick, R. E. *J. Chem. Phys.* **1962**, *37*, 307.
(34) Rusnak, L. L.; Jordan, R. B. *Inorg. Chem.* **1976**, *15*, 709.
(35) Hioki, A.; Funahashi, S.; Tanaka, M. *J. Phys. Chem.* **1985**, *89*, 5057.
(36) Inada, Y.; Ozutsumi, K.; Funahashi, S.; Soyama, S.; Kawashima, T.; Tanaka, M. *Inorg. Chem.* **1993**, *32*, 3010.
(37) Jordan, R. B. *Reaction Mechanisms of Inorganic and Organometallic Systems*; Oxford University Press: New York, 1991.

Table 1. Kinetic Parameters for Solvent Exchange of Mn^{2+}, Fe^{2+}, Co^{2+}, and Ni^{2+} in Water and Ethylenediamine

	solvent	Mn^{2+}	Fe^{2+}	Co^{2+}	Ni^{2+}
k_{ex}^{298}/	H_2O^a	2.1×10^7	4.4×10^6	3.2×10^6	3.8×10^4
s^{-1}	en[b]	1.7×10^6	4.3×10^4	5.4×10^3	2.0×10^c
$\Delta H^{\ddagger}$/	H_2O^a	32.9	41.4	46.9	56.9
kJ mol^{-1}	en[b]	24.7 ± 1.6	46.3 ± 1.4	56.5 ± 3.3	69 ± 3^c
$\Delta S^{\ddagger}$/	H_2O^a	5.7	21.2	37.2	32.0
J mol^{-1} K^{-1}	en[b]	-43 ± 5	-1 ± 4	16 ± 10	10 ± 11^c
$\Delta V^{\ddagger}$/	H_2O^a	−5.4	3.8	6.1	7.2
cm^3 mol^{-1}	en[b]	-0.6 ± 0.5^d	-1.2 ± 0.8^e	0.9 ± 0.9^f	$11.4 \pm 0.2^{c,g}$

[a] Reference 37 and references cited therein. [b] This work. [c] Reference 27. [d] At 278.4. [e] At 324.5 K. [f] At 332.4 K. [g] At 383 K.

change in k_{ex} and $\Delta H^{\ddagger}$ can be explained by the difference in the crystal field activation energy. Second, changes in sign of $\Delta V^{\ddagger}$ from positive to negative along the series from Ni^{2+} to Mn^{2+} accompanied by a decrease in $\Delta S^{\ddagger}$ are commonly observed except for DMF. The change in sign indicates a gradual changeover of mechanism from I_d to I_a along the series from Ni^{2+} to Mn^{2+}.[23] From the positive value of $\Delta V^{\ddagger}$ for DMF exchange on Mn^{2+}, it has been concluded that the steric bulkiness of DMF causes a less associative activation mode.[38]

A careful comparison of the kinetic parameters along the transition-metal(II) series for the en exchange with those for the monodentate solvent exchange[37] will disclose several characteristic features for the bidentate en exchange as follows; (i) The exchange rate constants for en are commonly smaller than those for the monodentate solvents for the corresponding metal ions, and the variation in k_{ex} from Ni^{2+} to Mn^{2+} is more drastic for the en exchange. Consequently, the difference in k_{ex} between en and monodentate solvents for Ni^{2+} is much greater than that for Mn^{2+}. (ii) The $\Delta H^{\ddagger}$ values for the en exchange decrease more drastically rather than those for the monodentate solvent exchange along the series from Ni^{2+} to Mn^{2+}. (iii) The en exchange tends to show more negative values of $\Delta S^{\ddagger}$ than those for the monodentate solvent exchange for the corresponding metal ions. (iv) The $\Delta V^{\ddagger}$ values for the en exchange do not indicate the mechanistic changeover along the series from Ni^{2+} to Mn^{2+} as observed for the monodentate solvent exchange.

The activation volume of 11.4 ± 2.0 cm^3 mol^{-1} for the en exchange on Ni^{2+} is comparable to those for the monodentate solvents, and thus the dissociative mechanism has been previously claimed.[27] For the en exchange on Mn^{2+}, the associative mode of activation is not supported by the fact that the presence of DMF added as a diluent does not affect the exchange rate. We can reasonably expect the dissociative-interchange (I_d) mechanism is more favorable for Co^{2+} and Fe^{2+} than for Mn^{2+} on the basis of the ionic radius and the t_{2g} orbital occupancy as reported for some monodentate solvents[23] while the $\Delta V^{\ddagger}$ values are close to zero.[39] The characteristic features of the en exchange (i)−(iv) seem to be mainly ascribed to the steric factors of en as a bidentate chelate.

Fortunately, a great number of crystal structural data are available to estimate the structure of the present en metal complexes. Because of the rigidity of the framework of $[M(en)_3]^{n+}$, the structure of the ground state in solution can be presumed from the crystal structures. Figure 3 shows the dependences of the N−N chelate bite distance in $[M(en)_3]^{n+}$ [40-56]

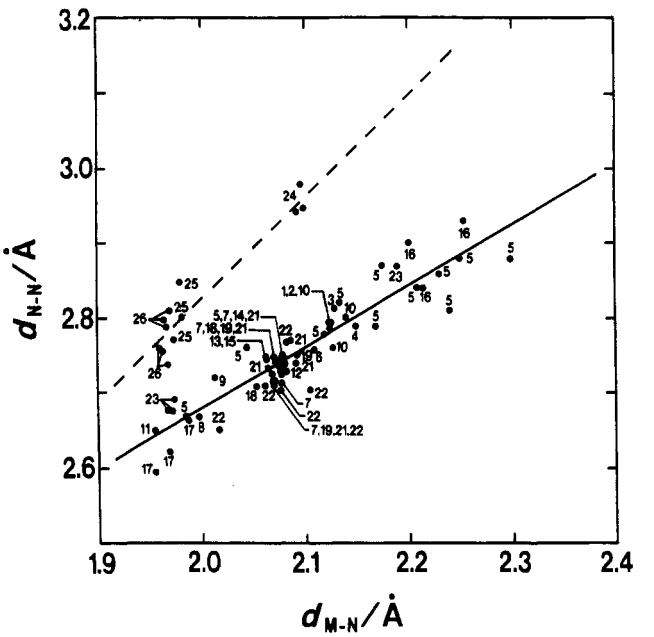

Figure 3. Plots of d_{N-N} versus d_{M-N} in $[M(en)_3]^{n+}$, $[M(tn)_3]^{3+}$, and $[M(NH_3)_6]^{3+}$. In $[M(en)_3]^{n+}$, M = Ni(II) (1),[40] Ni(II) (2),[41] Ni(II) (3),[42] Cu(II) (4),[42] Cu(II) (5),[43] Ru(III) (6),[44] Cr(III) (7),[45] Co(III) (8) and Cr(III) (9),[46] Ru(II) (10),[47] Co(III) (11) and Cr(III) (12),[48] Rh(III) (13),[49] Cr(III) (14) and Rh(III) (15),[50] Zn(II) (16),[51] Co(III) (17), Rh(III) (18), and Ir(III) (19),[52] Co(III) (20),[53] Cr(III) (21),[54] Cr(III) (22),[55] and Zn(II) (23).[56] In $[M(tn)_3]^{3+}$, M = Cr(III) (24)[57] and Co(III) (25).[58] In $[M(NH_3)_6]^{3+}$, M = Co(III) (26).[59] Two bond distances in the same chelate ring are averaged to give d_{M-N}. The dotted line represents the dependence of d_{N-N} on d_{M-N} ($d_{N-N} = 2^{1/2}d_{M-N}$) for the tn and ammine complexes, and the solid line represents the dependence for the en complexes.

and $[M(tn)_3]^{n+}$ (tn = trimethylenediamine)[57,58] and the distance between cis nitrogens in $[M(NH_3)_6]^{n+}$ [59] (d_{N-N}) on the M−N bond distance (d_{M-N}) in the corresponding complexes. The chelate bite angles in the en and tn complexes and the N−M−N angles for cis nitrogens in the ammine complexes (θ_{N-M-N}) are given as a function of d_{M-N} in Figure 4. The structural data used are listed in Table S7. The d_{N-N} in en complexes is actually elongated but decreases gradually from the distance of

(38) Ishii, M.; Funahashi, S.; Tanaka, M. *Chem. Lett.* **1987**, 871.
(39) We have preliminary data for the trimethylenediamine (tn) exchange in which the particular chelate strain is not expected because tn forms a six-membered chelate ring. The $\Delta V^{\ddagger}$ values for the tn exchange on Co^{2+} and Fe^{2+} are more positive, 6.6 ± 0.3 and 5.8 ± 0.4 cm^3 mol^{-1}, respectively.
(40) Haque, M.-U.; Caughlan, C. N.; Emerson, K. *Inorg. Chem.* **1970**, *9*, 2421.
(41) Jameson, G. B.; Schneider, R.; Dubler, E.; Oswald, H. R. *Acta Crystallogr.* **1982**, *B38*, 3016.
(42) Cullen, D. L.; Lingafelter, E. C. *Inorg. Chem.* **1970**, *9*, 1858.
(43) Bertini, I.; Dapporto, P.; Gatteschi, D.; Scozzafava, A. *J. Chem. Soc., Dalton Trans.* **1979**, 1409.
(44) Peresie, H. J.; Stanko, J. A. *J. Chem. Soc., Chem. Commun.* **1970**, 1674.
(45) Raymond, K. N.; Corfield, P. W. R.; Ibers, J. A. *Inorg. Chem.* **1968**, *7*, 1362.
(46) Whuler, P. A.; Brouty, C.; Spinat, P.; Herpin, P. *Acta Crystallogr.* **1976**, *B32*, 194.
(47) Smolenaers, P. J.; Beattie, J. K.; Hutchinson, N. D. *Inorg. Chem.* **1981**, *20*, 2202.
(48) Whuler, P. A.; Brouty, C.; Spinat, P.; Herpin, P. *Acta Crystallogr.* **1975**, *B31*, 2069.
(49) Whuler, P. A.; Brouty, C.; Spinat, P.; Herpin, P. *Acta Crystallogr.* **1976**, *B32*, 2238.
(50) Whuler, P. A.; Brouty, C.; Spinat, P.; Herpin, P. *Acta Crystallogr.* **1976**, *B32*, 2542.
(51) Cernak, J.; Chomic, J.; Dunaj-Jurco, M.; Kappenstein, C. *Inorg. Chim. Acta* **1984**, *85*, 219.
(52) Hoffmann, S. K.; Hodgson, D. J.; Hatfield, W. E. *Inorg. Chem.* **1985**, *24*, 1194.
(53) Veal, J. T.; Hodgson, D. J. *Inorg. Chem.* **1972**, *11*, 597.
(54) Whuler, P. A.; Spinat, P.; Brouty, C. *Acta Crystallogr.* **1978**, *B34*, 793.
(55) Whuler, P. A.; Brouty, C.; Spinat, P.; Herpin, P. *Acta Crystallogr.* **1977**, *33B*, 2877.
(56) Podberezskaya, N. V.; Borisov, S. V. *Zh. Strukt. Khim.* **1971**, *12*, 1114.
(57) Jurnak, F. A.; Raymond, K. N. *Inorg. Chem.* **1974**, *10*, 2387.
(58) Nagao, R.; Marumo, F.; Saito, Y. *Acta Crystallogr.* **1973**, *B29*, 2438.
(59) Clegg, W. *Acta Crystallogr.* **1985**, *C41*, 1164.

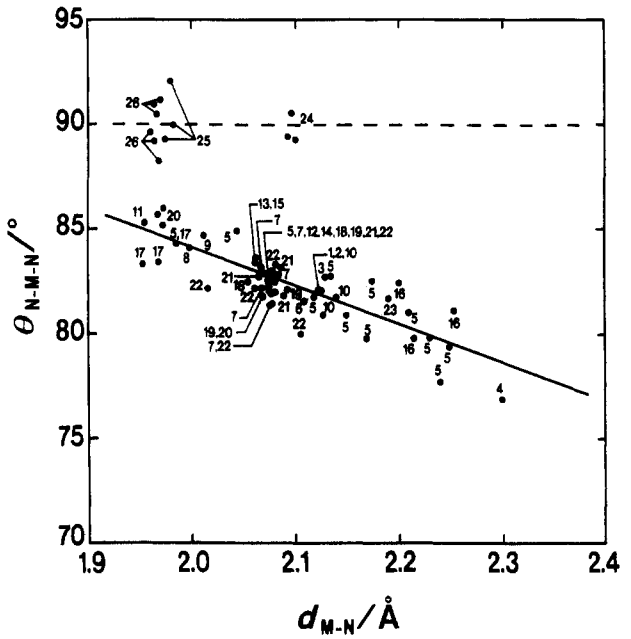

Figure 4. Plots of θ_{N-M-N} versus d_{M-N} for $[M(en)_3]^{n+}$, $[M(tn)_3]^{3+}$, and $[M(NH_3)_6]^{3+}$. Numbering is in accordance with that in Figure 3. The dotted line represents the dependence of θ_{N-M-N} on d_{M-N} (θ_{N-M-N} = 90°) for the tn and ammine complexes, and the solid line represents the dependence for the en complexes.

Scheme 1

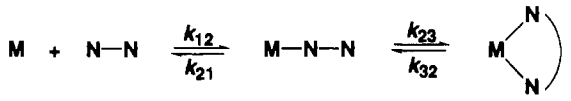

$2^{1/2}d_{M-N}$, which is the distance in the case of a regular octahedral complexes, and θ_{N-M-N} also decreases from the regular angle of 90° with increase in d_{M-N}, while the regular octahedron is maintained in $[M(tn)_3]^{n+}$ and $[M(NH_3)_6]^{n+}$. These findings indicate that the distortion from octahedral geometry for the complexes with a long M−N bond distance is due to chelate strain.

Since the σ bonding mainly operates on the M−N bond in the case of an amine nitrogen donor, the strength of the bond is sensitive to the degree of overlap of the σ orbitals, which is determined by observing the M−N−C bond angle (θ_{M-N-C}). The relationship between θ_{M-N-C} and d_{M-N} is shown in Figure 5. While no pronounced decrease in θ_{M-N-C} is observed for the relatively small metal ions with d_{M-N} shorter than ca. 2.1 Å, there is a considerable decrease in θ_{M-N-C} for the complexes with longer d_{M-N}. Therefore, the chelate strain is not completely compensated only by the decrease in d_{N-N} and/or θ_{N-M-N} in the larger metal complexes, and an increase in d_{M-N} compels θ_{M-N-C} to decrease and weakens the M−N bond.

On the basis of the steric effects described above, we will consider the origin of the kinetic chelate effect. Scheme 1 shows the chelate formation process for en complexes and the formation constant is given by eq 5. Generally, the chelate

$$K_f = k_{12}k_{23}/k_{21}k_{32} \quad (5)$$

effect observed as a large formation constant can be partially ascribed to a large ring-closing rate, k_{23}, because of a local concentration effect. On the other hand, Jordan has claimed that the chelate effect comes from an unexpectedly slow rate for the chelate ring opening, k_{32}, rather than a large k_{23}.[37,60] From consideration of the structure of the ground state, we cannot expect a significant difference in the binding energy of the M−N bond between $[M(en)_3]^{n+}$ and $[M(NH_3)_6]^{n+}$ in the complexes with d_{M-N} shorter than 2.1 Å. In fact, the M−N bond distances for $[Co(en)_3]^{3+}$,[46,48,52,53] $[Co(tn)_3]^{3+}$,[58] and $[Co(NH_3)_6]^{3+}$ [59] similarly range between 1.95 and 2.00 Å. However, in the transition state for the chelate ring opening, the elongated M−N bond in the chelate complexes should decrease the M−N−C bond angle and highly weaken the σ bonding compared to the case of complexes with monodentate ligands. The relatively large enthalpy loss for the chelate complexes in the transition state is responsible for the large activation energy for the chelate opening (Figure 6a,b). The entropy change may also contribute to the difference in activation energy between the complexes with bidentate and monodentate ligands. If the degree of dissociation of the leaving ligand in the transition state is comparable, the monodentate ligand acquires a larger degree of freedom than the partially bound chelate ligand. These differences in enthalpy and entropy of activation between the complexes with bidentate and monodentate ligands should cause the difference in activation energy for the k_{32} path (Figure 6a,b). This is the origin of the smaller k_{32} value and, consequently, the large K_f for the en chelate formation process, i.e., the chelate effect.

The decrease in θ_{M-N-C} for the relatively large metal ions with d_{M-N} longer than 2.1 Å implies that the ground state is less stable due to the enthalpy loss for the large metal ions. Thus, this means that the activation energy for the k_{32} path should become smaller in comparison with those of small metal ions (Figure 6b,c). We may call this phenomenon the "kinetic chelate strain effect".

The explanation described above can be applied to the solvent exchange reaction to compare the bidentate chelate solvent, en, with monodentate solvents. Because the dissociative or dissociative-interchange mechanism is operative for the en exchange on Ni^{2+},[27] Co^{2+}, Fe^{2+}, and Mn^{2+}, the effect of an entering solvent does not seem to be so significant. Furthermore, the difference in the steric effect between entering bidentate and monodentate solvents may be negligible because the bidentate solvent approaches a metal center through one terminal donor atom. Therefore, in the case of relatively small metal ions, the slower rate for the en exchange is expected due to the highly activated transition state for the chelate ring opening. It is deduced from all the data for the M−N bond distances that the difference between an M−N bond distance and a metal ion radius (r_M),[61] $d_{M-N} - r_M$, is ca. 1.29 Å for each metal ion. Accordingly, in spite of lack of the crystal structural data for Co^{2+}, Fe^{2+}, and Mn^{2+}, we can estimate the d_{M-N} for the metal ions Co^{2+}, Fe^{2+}, and Mn^{2+} to be 2.18, 2.21, and 2.26 Å from their ion radii (0.89, 0.92, and 0.97 Å),[61] respectively. Moreover, we can predict the values of d_{N-N}, θ_{N-M-N}, and θ_{M-N-C} for each metal ion. For example, $[Mn(en)_3]^{2+}$ may have a distorted octahedral geometry with d_{N-N} = 2.8−2.9 Å, $\theta_{N-M-N} < 80°$, and $\theta_{M-N-C} \simeq 105°$. In this way, a decrease in M−N−C angles is expected in the order $Co^{2+} > Fe^{2+} > Mn^{2+}$, while no distinguishable decrease is observed for Ni^{2+} according to the crystal structures.[40,41] As stated above, the distortion in the ground state cancels the chelate effect and causes an increase in k_{ex} and a decrease in $\Delta H^{\ddagger}$. In conclusion, the chelate strain effect which arises from the increase in M−N bond distance results in characteristics i and ii. In addition, the entropy loss for an entering en solvent is comparable to that for monodentate solvents in a similar reaction mechanism, while the gain of entropy for a leaving en solvent which is bound on the other side is much smaller than

(60) Jordan, R. B. *Inorg. Chem.* **1976**, *15*, 748.

(61) Shannon, R. D. *Acta Crystallogr.* **1976**, *A32*, 751.

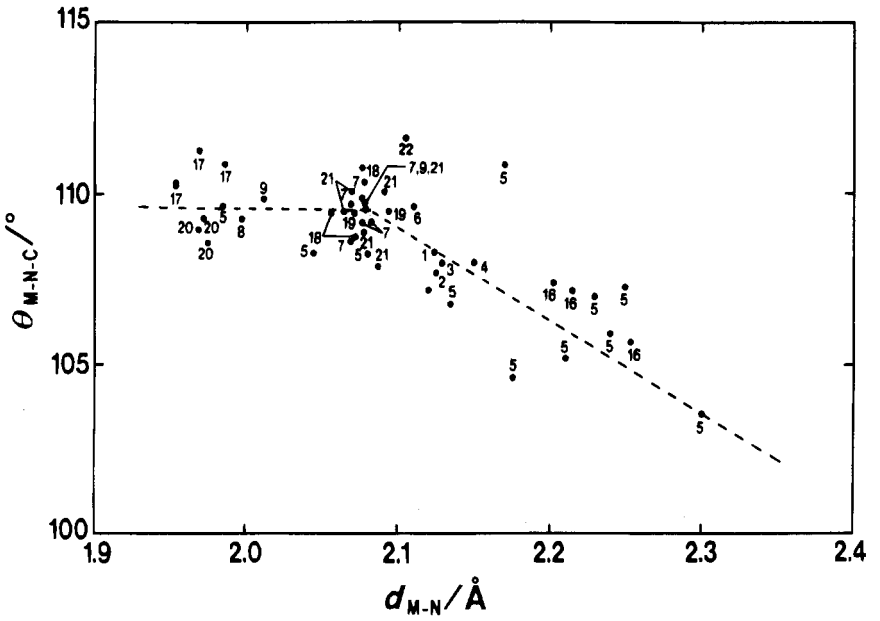

Figure 5. Plots of θ_{M-N-C} versus d_{M-N} for $[M(en)_3]^{n+}$. Two M−N−C angles in the same chelate ring are averaged to give θ_{M-N-C}. Numbering is in accordance with that in Figure 3.

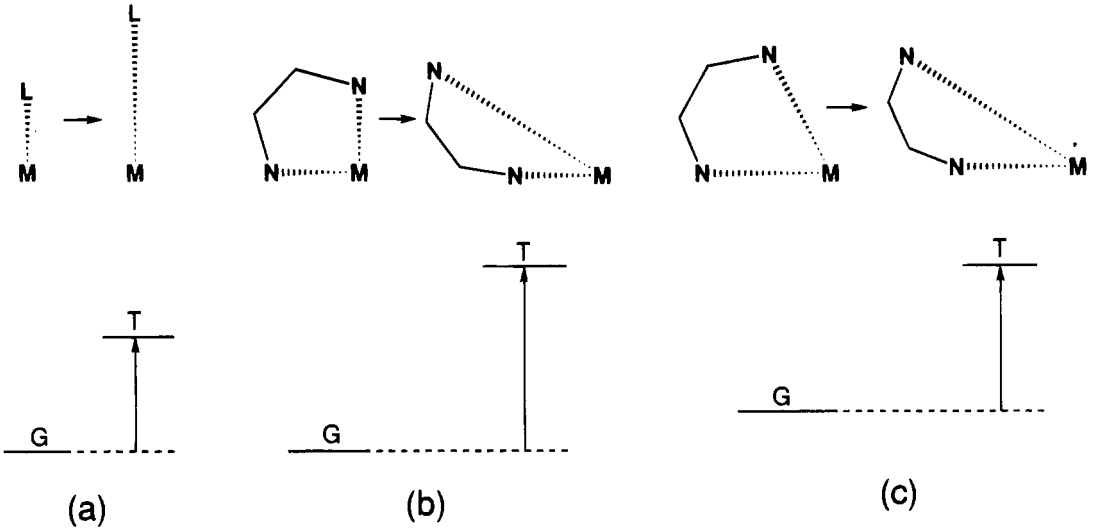

Figure 6. Schematic diagram for relative energy change between the ground state (G) and the transition state (T) for dissociation of a monodentate ligand L (a), ring opening of an en chelate with a short bond distance (b), and ring opening of an en chelate with a long bond distance (c).

that for monodentate solvents. This may be an explanation for characteristic iii.

In the transition state for monodentate solvent exchange, both entering and leaving solvent molecules must be equivalent according to the principle of microscopic reversibility. This compels the leaving solvent to vary the direction of bonding in order to relieve the steric repulsion between the entering and leaving solvents especially for solvent exchange with an associative activation mode. This repulsion is also operative in the chelate solvent system even if the entering and leaving solvents may not be equivalent. From a structural point of view, the N−N distance of the leaving en solvent would be diminished in the associative mechanism to make an open space which can accommodate the entering donor atom. In fact, a decrease in the N−N distance is possible only by the rotation around the C−C bond, and the minimum N−N distance is formed by the minimum torsion angle of two N−C bonds about the C−C axis. However, if the torsion angle approaches 0°, a sterically unfavorable conformation results because of the eclipsed structure. This limits the shortening in the N−N distance and the decrease in the chelate bite angle and indicates that it is very difficult to make the space for the approach of the entering solvent without an extension of bonding for the leaving donor atom. Consequently, the reaction mechanism for the en solvent exchange on the first-row transition-metal(II) ions is restricted to a dissociative or a dissociative-interchange mechanism. This fact is reflected in characteristic iv.

Acknowledgment. This research was supported by Grants-in-Aid for Scientific Research (Nos. 04403011 and 06640779) from the Ministry of Education, Science, and Culture of Japan. S.A. gratefully acknowledges receipt of a grant from the Kurata Foundation.

Supplementary Material Available: Compositions of sample solutions (Table S1), NMR line-broadening data at various temperatures for Co^{2+} (Table S2), Fe^{2+} (Table S3), and Mn^{2+} (Table S4), values of $\Delta H^{\ddagger}$, $\Delta S^{\ddagger}$, C_M, E_M, C_0, E_0, and C_ω (Table S5), NMR line-broadening data at various pressures (Table S6), structural data for $[M(en)_3]^{n+}$, $[M(tn)_3]^{3+}$, and $[Co(NH_3)_6]^{3+}$ (Table S7), and the temperature dependences of $(T_{2P}P_M)^{-1}$ for Co^{2+} (Figure S1), Fe^{2+} (Figure S2), and Mn^{2+} (Figure S3) (28 pages). Ordering information is given on any current masthead page.

IC941263V